Energy and Buildings 50 (2012) 74–80

Contents lists available at SciVerse ScienceDirect

Energy and Buildings

journal homepage: www.elsevier.com/locate/enbuild

Study of the influence of roof insulation involving local materials on cooling loads of houses built of clay and straw

David Y.K. Toguyeni[a], Ousmane Coulibaly[a], Abdoulaye Ouedraogo[b], Jean Koulidiati[a], Yvan Dutil[c,*], Daniel Rousse[c]

[a] UO-UFR/SEA – Laboratoire de physique et de chimie de l'environnement (LPCE), 03 BP 7021 Ouagadougou 03, Burkina Faso
[b] UO-UFR/SEA – Laboratoire d'énergie thermique et renouvelable (LETRE), 03 BP 7021 Ouagadougou 03, Burkina Faso
[c] Chaire industrielle en technologie de l'énergie et efficacité énergétique (T3E), Ecole de Technologie Supérieure, Département de Génie mécanique, 1100 rue Notre-Dame, Ouest Montréal, Canada

ARTICLE INFO

Article history:
Received 5 October 2011
Received in revised form 20 February 2012
Accepted 10 March 2012

Keywords:
Hot plate method
Roof influence
Clay–straw mixture
TRNSYS model
Air conditioning load
Dry tropical climate

ABSTRACT

This paper presents an investigation of the influence of local insulated roofing materials used in Burkina Faso on air conditioning loads of typical individual houses located in dry tropical climates. The walls are made of a composite clay–straw mixture whereas the insulated materials are made of red wood, white wood, and two assembled insulated panels. The thermophysical properties of the insulating materials as well as the clay–straw composite have been studied, utilizing an experimental apparatus based on the hot plate method. The values of the thermophysical properties obtained are in the same range as those published in the literature. Afterward, the house has been modeled using TRNSYS together with the climatic data of Ouagadougou. This simulation shows that the clay–straw mixture reduces the air conditioning load by about 8% compared to clay walled houses. As for the roof, the study indicates the influence of the insulated materials on the air conditioning load. Hence, a 1.5 cm thick insulator made of red wood induces a saving of energy about 6.2% and 12.1% for an insulation panel made of natural fiber and a lime–cement mixture on the air conditioning load.

1. Introduction

In tropical countries, buildings were designed until today without any consideration for their energy efficiency. This results in high cooling loads for owners unacquainted with the proper use of energy. For instance, in Burkina Faso, the energy consumption of public buildings, including the operation of air conditioning units, is estimated at 30 GWh/year. This corresponds to a financial cost estimated at 3.4 billion francs CFA/year or 5.2 million euros [1]. These financial charges are very important in a country such as Burkina Faso for which the GNG/cap is low. In the hot climate of Bukina Faso (~3900 cooling degree-day [2]), air conditioning is a major contributor to the energy load of a building. With the expected larger air conditioning market penetration combined with the increase in temperature due to climate change [3], this financial burden will grow further if nothing is done to mitigate it. Thus, promotion of building insulation materials to improve energy efficiency in housing is essential.

As part of its Programme International de Soutien à la Maîtrise de l'Énergie (PRISME), l'Institut de l'énergie et de l'environnement de la Francophonie (IEPF), a subsidiary body of the Agence Intergouvernementale de la Francophonie, provided recommendations for improving energy efficiency in buildings in tropical regions. These studies [4,5] have identified potential savings on energy costs that varies from country to country from 30 to 45%. According to these studies, most of the potential energy savings can be found in air conditioning installations that represent more than 60% of exploitable negawatt sources. In [3], the Institute reported that, in tropical climates, the roof is responsible for approximately 30% of heat gain inside the building. Recently, work by Ouedrago et al. [6] have focused on the design of a bioclimatic roof to provide passive cooling optimal habitat in Ouagadougou, the capital of Burkina Faso that has a hot and dry tropical climate. The search for optimum operating conditions of this system led the authors to analyze the influence on the air temperature and air flow rate circulated by natural convection in the roof and the walls of the habitat. Other parameters of interest for the habitat are the slope of the roof and the stack height. The study showed that the habitat must be oriented north-south, with an ideal 50° pitched roof and chimney height that should be 0.15 m.

* Corresponding author. Tel.: +1 418 653 2910.
E-mail addresses: togyen@univ-ouaga.bf (D.Y.K. Toguyeni), ousmane.coulibaly@univ-ouaga.bf (O. Coulibaly), abdoulay@univ-ouaga.bf (A. Ouedraogo), jean.koulidiati@univ-ouaga.bf (J. Koulidiati), yvan@t3e.info (Y. Dutil), daniel@t3e.info (D. Rousse).

0378-7788/$ – see front matter © 2012 Elsevier B.V. All rights reserved.
doi:10.1016/j.enbuild.2012.03.021

Nomenclature

Rc_1	contact resistance between the hot plate and the sample material
Rc_2	contact resistance between the sample material and the reference material
m	thermocouple + hot plate mass
c	thermocouple + hot plate thermal capacity
E	effusivity of the sample material
e	sample thickness
a	diffusivity of the sample material
p	Laplace multiplier
q	auxiliary variable
S	area of the hot plate
t	time
T	temperature

Greek letter

ϕ_0	power dissipated in the hot plate
θ_0	Laplace transform of $T_0(t) - T_0$ $(t=0)$
θ_3	Laplace transform of $T_3(t) - T_3$ $(t=0)$

To maximize to rate of the adoption of energy efficiency behaviors, it is essential that the proposed solutions involve a minimal change to the present day practices. Hence, this work focuses on technical solutions that could be implemented as a simple modification of actual construction practices and as possible retrofit solutions for existing housing.

Given the fact that clay is the most available and widely used building material by the average household in Burkina Faso (this is also a common practice in many parts of the world), this research was conducted on the influence of the presence of straw on the insulating properties of clay based construction materials. To alleviate the issue of the weak mechanical strength of clay, the traditional technique is to make a concrete base and add slender mortar surface coatings to the wall. In addition, it should be noted that the addition of fibers, in this case straw, improves the overall mechanical properties of the clay [7]. It is also recognized that the clay has a high thermal inertia. It is this property that imposes the use of dynamic building simulation codes as the response time in storage lags the heat load from the environment.

In the present study, the local materials that can be used as roof insulation were also examined. These are the red wood and white wood, which are two tropical species known also respectively as Wa wa Samba (*Triplochiton scleroxylon*) and African mahogany (*Khaya ivorensis*). Two insulating panels 1 and 2 made from natural fibers of Burkina Faso (*Hibiscus sabdariffa*) and lime–cement mixtures were also considered as potential alternatives.

2. Characterization of samples by the method of hot plate

In this work, the first measurements of effusivity and thermal conductivity using a device such as the hot plate (Fig. 1) were carried out for the above mentioned materials.

2.1. Experimental set-up

In Fig. 1, the thin electrical heater (shown in dark) is squeezed between two identical samples of the material to be characterized (in light gray). This assembly is maintained together by two external layer of insulating material (in white) for which the properties are known. The temperatures T_0 (on symmetry axis), T_1 (at the boundaries between the heater and the material), T_2 (at the boundaries between the material and the insulation), and T_3 (within the insulating layer) are monitored during the experience. The electric power is measured in terms of the electric current I in amps.

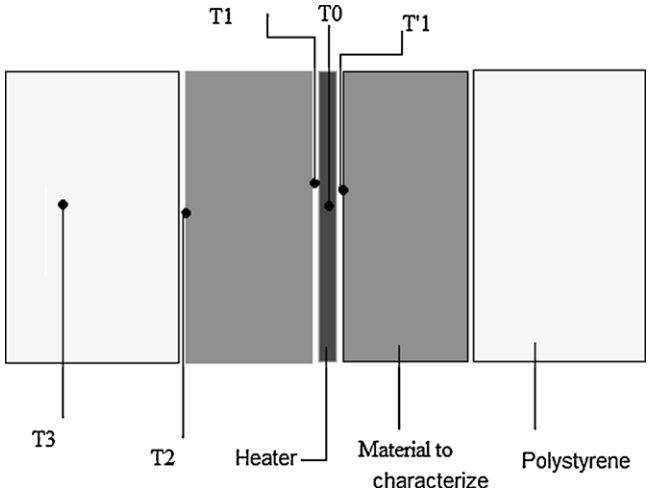

Fig. 1. Schematic of the experimental set-up.

A uniform heat flux is imposed at the interface of two samples of this symmetrical arrangement and along the extension in the direction perpendicular to the interface makes the problem one-dimensional at mid-height. The samples are then treated as an infinite medium in the y-direction (height) when the ratio of length to the thickness of the heating element is greater than 20. Moreover, the side faces of the two samples are isolated such as the transfer can be considered unidirectional. The temperature response over time is measured with J-type thermocouples. The method for characterization and estimation are based on the work of Jannot et al. [8]: this one consist of the application of the method of quadrupoles and the utilization of the method for calculating Sthefest inverse Laplace transforms. The parameter determination is then carried out by the application of Newton's method for minimizing the squared deviations between experimental and theoretical thermograms.

2.2. Modeling the hot plate and estimation methods

The model using the formalism of the quadrupole [8] is described herein. This formalism is used to combine the effect of each component on propagation of the heat through the experimental setup. In this case, the contribution of the thermal inertia of thermocouples and the contact resistance of the plate are taken into account within the contribution of the insulation material itself. We can thus write:

$$\begin{bmatrix} \theta_0 \\ \dfrac{\phi_0}{2p} \end{bmatrix} = \begin{bmatrix} 1 & 0 \\ \dfrac{mc}{2}p & 1 \end{bmatrix} \begin{bmatrix} 1 & Rc_1 \\ 0 & 1 \end{bmatrix} \begin{bmatrix} A & B \\ C & D \end{bmatrix} \begin{bmatrix} 1 & Rc_2 \\ 0 & 1 \end{bmatrix} \begin{bmatrix} \theta_3 \\ E_i S\sqrt{p}\theta_3 \end{bmatrix} \tag{1}$$

with the following term describing the contribution of the insulation material:

$$\begin{bmatrix} A & B \\ C & D \end{bmatrix} = \begin{bmatrix} \cosh(qe) & \dfrac{1}{\lambda q S}\sinh(qe) \\ \lambda q S \cosh(qe) & \cosh(qe) \end{bmatrix}, \quad \text{and } q = \sqrt{\frac{p}{a}} \tag{2}$$

Jannot et al. [8] showed that after modeling by use of the method of quadrupoles in conjunction with the Sthefest method for a semi-infinite medium, the temperature difference $T_0(t) - T_0(0)$ can be calculated by:

$$T_0(t) - T_0(0) = \frac{\phi_0}{2}\left[Rc - \frac{mc}{2(E \cdot S)^2}\right] + \frac{\phi_0}{ES\sqrt{\pi}}\sqrt{t} \tag{3}$$

From Eq. (3), it can readily be observed that $T_0(t) - T_0(0)$ vs $\sqrt{t}$ is a straight line for which the slope ($\phi_0/E \cdot S\sqrt{\pi}$) allows for the determination of the thermal effusivity.

The first term of Eq. (3) is not useful to determine the effusivity since it is sensitive to contact resistance and thermal properties of the thermocouple. However, this term become negligible at later times compared to the second term.

To apply this method of estimation, one must ensure that the assumption of a semi-infinite medium is valid. The principle for the estimation method is to use the first part of the thermogram [0,t_1] to determine the parameters E, Rc_1 and $m{\cdot}c$ as described above. Time t_1 can be identified by plotting $T_0(t) - T_0(0)$ vs t. It is the time corresponding to the threshold for which the plot is linear. Overall, the main source of uncertainty is the value of the density of heat flow. There is a systematic uncertainty common to all measurements, which comes from current and resistance uncertainties estimated at 4.1%. Uncertainty in area is estimated conservatively at 3.6%. The last contribution is the relative error of the slope, which varies between 3% and 6%. Overall, the uncertainties on effusivity values range between 6 and 8%.

In steady state, the temperature difference is constant between the different faces. One can then estimate the thermal conductivity using the following equation:

$$\lambda = \frac{\phi_0 \cdot e}{S\Delta T} \tag{4}$$

ΔT and e being respectively, the temperature difference and the thickness of the sample. Uncertainty on conductivity accounts for the flux and surface area uncertainties used for the determination of effusivity. Uncertainty on temperature differences between each side is 10% maximum, while uncertainties on thickness is 5% for wood material and 10% for insulation panel due to the surface roughness. Combined together these results translate into an uncertainties between 13 and 15% on conductivity.

2.3. Thermophysical properties of characterized materials

Fig. 2 presents experimental data and adjusted model (based on the Eq. (3)) curves of ΔT vs $\sqrt{t}$ transient thermal response for the insulation panel 1. Adjusted model is based on the simultaneous least square fit for the three applied heat fluxes, which correspond to electric current of 0.25, 0.35 and 4.5 A. Optimization of the fit is achieved by the Newton method. Only the data taken after 35 s of heating are used to avoid the unstable behavior in the first few seconds of the experiment (the thick continuous line on the graph). This can be explained by the water vapor outgassing, which is important for this porous material. Nevertheless, Fig. 2 shows an excellent agreement between calculations and experiments ($R > 0.99$).

Note that the white wood (density equal to 408 kg/m^3) and red (density equal to 613 kg/m^3) are two tropical species available locally. As for the insulating panels 1 and 2, they were made by Jean Hugues Thomassin from l'École Supérieure des Ingénieurs de Poitiers (ESIP) from natural fibers of Burkina Faso (Hibiscus sabdariffa) and lime–cement mixtures. These materials were sent to the ECPA (Laboratoire de physique et de chimie de l'environnement) for their thermal characterization. It should be noted that parallel research conducted at the ECPA allowed comparison of the thermophysical properties of the panels from alternate experimental methods and that use herein. The relative differences are in the order of 8% [10].

Table 1 indicates the thermophysical properties of materials that were extracted from the measurements and determined by the method described above. These results can be compared with those of Izard [9]. However, the adopted properties of mortar coating, concrete and asphalt are taken from the literature [5].

It should be noted that the heat capacity of the clay walls has been greatly enhanced by the presence of straw. This reflects the fact that straw is strongly hydrophilic. Tests were carried out in summer when moisture levels in air are very high (RH ≈ 95%). In consequence, water content (with a high heat capacity) of the straw–clay composite is increased. Given the particular composition of the mixture, it is not really possible to make a direct comparison with previous studies [7,11,12]. However, the observed properties, especially thermal conductivity, are of the same order of magnitude.

3. Modeling with TRNSYS 16.1

To illustrate the impact of the inclusion of local materials in the building envelope on the cooling loads, a typical clay–straw house has been modeled in TRNSYS, based on the works of Al-Ajmi and Hambi [13], Annabi et al. [14], Shariah et al. [15], and Diez-Webster et al. [16].

3.1. Building description

The model implemented in TRNSYS 16.1 [17] is that of a standard house for residential use with a floor area of 50.02 m^2 with a south facing facade of 9.30 m wide by 3 m high. It is a standard one storey building involving two bedrooms, a living room, and a bathroom. It was built under the project 10,000 housing units by CEntre de GEstion des CItés (CEGECI) in Ouagadougou, Burkina Faso. The building configuration is depicted in Fig. 3.

The walls of the building are assumed to be made of clay or clay-coated straw with a mortar coating inside and outside. Fig. 4 schematically shows the two types of wall arrangements that were used. For each arrangement the core of the wall is made of 20 cm thick clay. In Fig. 4a, two mortar coatings 2.5 cm thick are added on each side of the core. A white paint is used on the inside and dark yellow paint on the outside. For aesthetics purposes, a clay coating is often used inside this type of habitat instead of concrete (Fig. 4b). That is why simulations with this type of inner coating were conducted for comparison with the interior coating made of mortar.

The floor is a 15 cm thick concrete slab. The doors are made of wood within a double steel frame. The windows are made of a single 4 mm thick glazing within a steel frame. Window conductance without the boundary layer resistance is equal to 5.7 W m^{-2} K^{-1} and solar heat gain coefficient is equal to 0.85. The roof concrete slab is 22 cm thick and covered with an asphalt sealing. Effects of red wood, white wood and insulation panels 1 and 2 on the cooling loads are analyzed.

This building has a considerable thermal mass which will lead to a damping of the amplitudes of internal temperature fluctuations with a phase shift of the latter compared to those from outside. This situation tends to increase the thermal comfort for the occupant, which in turn reduces the cooling needs. This situation imposes the use of a dynamic model to correctly describe the thermal behavior.

The simulations are performed over a complete year with a time step of 1 h (0–8760 h) using a typical multizone building (here a Type 56 building, characteristic of buildings found in the area). To get a more refined modeling of the habitat with respect to its real use, the entire space has been divided it into six areas described in TRNSYS (that is Living room, Terrace; Clearance; Bedroom 1 and 2; Bathroom). The meteorological data METEONORM for Ouagadougou proposed in version 16.1 of TRNSYS have been used for this simulation.

3.2. Internal charges and air conditioning system

According to the bioclimatic diagram of Givoni [18], the comfort zone lies between temperatures ranging from 20 to 27 °C, but

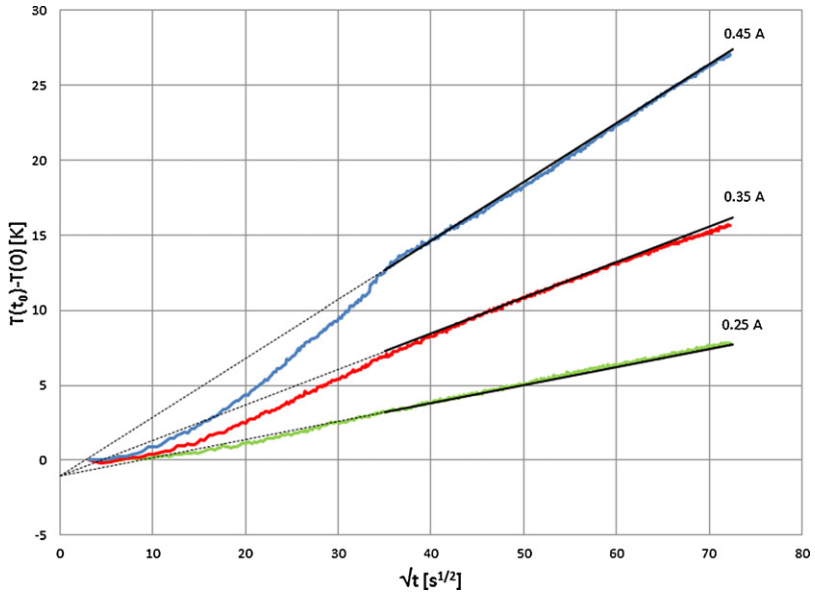

Fig. 2. Experimental data and model of the transient thermal response of the insulating panel 1.

the upper limit decreases, when the relative humidity exceeds 50% down to 24 °C. Another study conducted in the Ivory Coast showed that in dry tropical climates, interior comfort conditions are obtained for a dry bulb temperature of 26.5 °C and a relative humidity of 50% [14]. Hence, here, the thermal comfort zone is consequently defined by a dry bulb temperature between 26 and 27 °C and a relative humidity between 50 and 55%. This condition is then consistent with the study of Givoni [18].

For the purpose of simulations, the air conditioner is assumed to be turned on when the indoor temperature rises above 26 °C with a relative humidity of 50%. Ventilation and infiltration are set at one volume per hour. Due to their compact nature, the walls are naturally airtight. Scenarios for weekdays and weekend uses for the bedrooms and living room have been created. The number of occupants is four in the living room and two in each bedroom. For lighting, a fluorescent lamp whose power is 8 W is used in each room [5]. The living room holds a television (60 W) and a refrigerator (70 W) with a duty cycle of 100% and a DVD player (150 W) with load factor of 40% [5]. Cooking does not bring additional charges as it is normally done outdoors. These are standard figures for such a unit in Ouagadougou.

4. Simulation results and discussion

Fig. 5 compares the monthly thermal load of the clay wall to a wall made with a clay–straw composite both involving a non insulated roof. It presents the total heat load on the building in kW h with respect to the time of the year (here in months). As expected, the wall of clay–straw consumes less energy than the wall made entirely of clay; the relative difference being 7% over the year. Moreover, this difference is larger for the warmer months, March–June (see Fig. 5), which will impact the peak power consumption. This might allow using a smaller cooling system, bringing additional savings.

The effect of roof insulation on the annual charge for a wall of clay and clay–straw is given in Fig. 6. It presents the total heat load on the building in kW h with respect to several cases: non insulated roof, red wood insulation, white wood insulation, and two

Table 1
Materials properties.

Building component	Materials	Thickness (m)	Thermal conductivity (W m^{-1} K^{-1})	Density (kg/m^3)	Thermal capacity (J kg^{-1} K^{-1})
Clay–straw wall	Mortar coatings	0.025	0.87	2200	1050
	Clay coating (interior)	0.025	2.12	2026	658
	Case 1: clay wall (0%)	0.200	2.12	2026	658
	Case 2: straw–clay wall (3%)	0.200	0.53	1796	2202
Roof 1	Concrete	0.22	1.75	2100	653
	Roof seal (bitumen)	0.005	0.17	1050	1000
Roof 2	White wood (LPCE)	0.015	0.22	359	772
	Concrete	0.22	1.75	2100	653
	Roof seal (bitumen)	0.005	0.17	1050	1000
Roof 3	Red wood (LPCE)	0.015	0.31	595	830
	Concrete	0.22	1.75	2100	653
	Roof seal (bitumen)	0.005	0.17	1050	1000
Roof 4	Insulation panel 1	0.020	0.2	386	455
	Concrete	0.22	1.75	2100	653
	Roof seal (bitumen)	0.005	0.17	1050	1000
Roof 5	Insulation panel 2	0.020	0.13	349	705
	Concrete	0.22	1.75	2100	653
	Roof seal (bitumen)	0.005	0.17	1050	1000

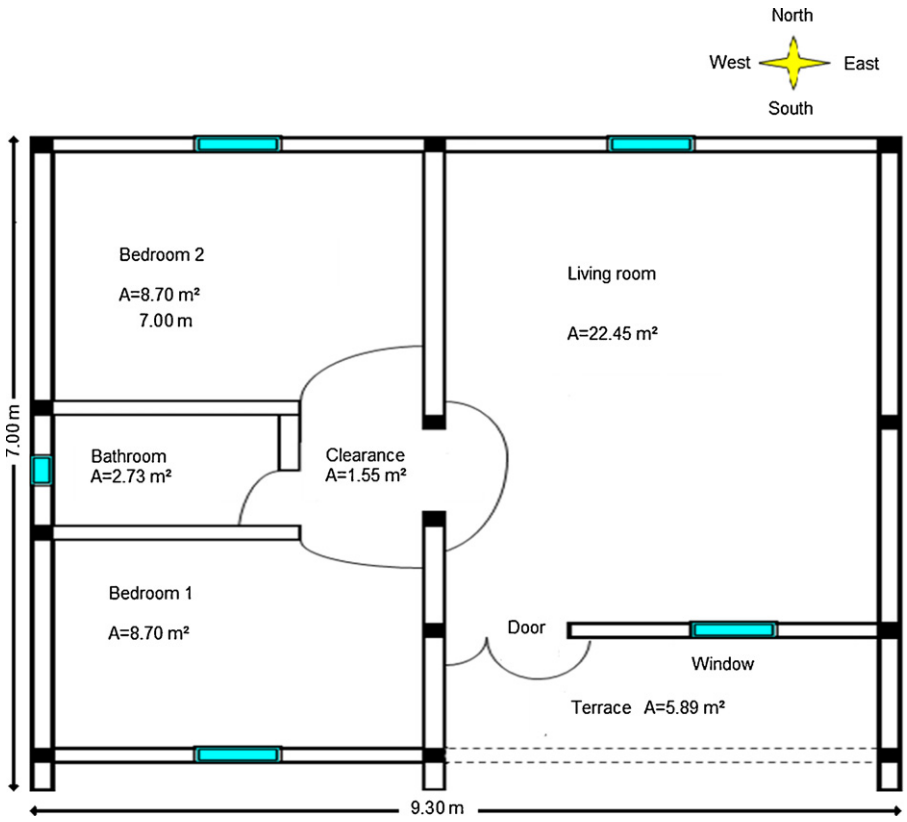

Fig. 3. Floor plan of the investigated building with orientation, dimensions, and surface areas.

types of insulation panels as discussed previously. The differences in annual expenses are about 8% (average) between the wall of clay and the clay–straw mix. To take handle the uncertainties in the evaluation of the thermophysical properties of the material, several simulations were carried out using the maximum and minimal possible values for such properties. For the worst case combination, the energy discrepancy is equal to 5% and 9%.The best roof insulation is obtained with insulation panel 2. For roof insulation 1.5 cm thick, changing from red wood to insulation panel 2 lowers expenses by 6.2–12.1%. The error on these values reaches a maximum of ±2.6%. Overall, energy consumption is reduced by 18.4% with inclusion of straw combined with a roof insulation made of panel 2 compared with the reference house with walls made of pure clay.

Since the simulation results demonstrate that a building envelope made of a 3% clay–straw mix is more efficient than one involving pure clay, the former was investigated to obtain the values of global heat gain for the whole year for various wall and roof configurations. In addition, interior coating of mortar improves only slightly the performance of the building envelope compared to a coating of clay. Since this is the most efficient configuration, we will use it for our subsequent analyses.

For each case simulated with interior mortar coating, as shown in Fig. 6. Table 2 provides the breakdown room by room of their separate heat loads. It is clear that the living room with its facades on the east, north and south, is the building's space in which the influence of the roof is most pronounced. The relative differences between the cases with non insulated roof varies from −9.3% to

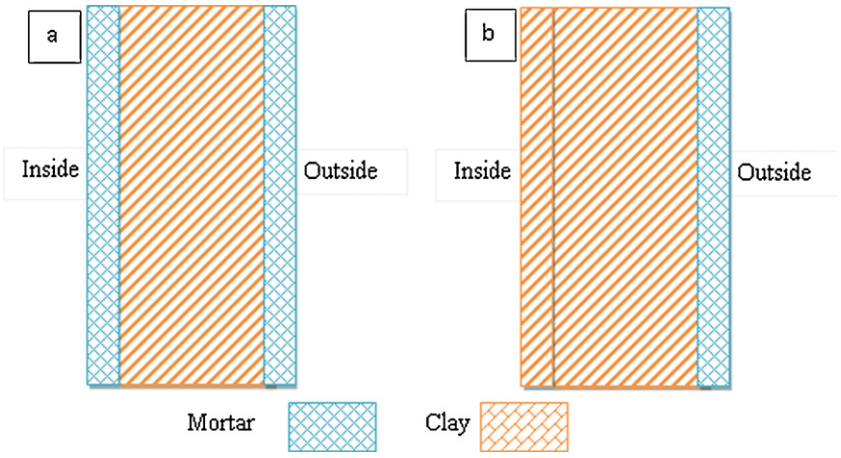

Fig. 4. Wall structure involving a 20 cm thick core: (a) both wall coatings are in made of 2.5 cm of mortar; (b) the interior coating is in clay, the exterior coating is in mortar.

Table 2
Sensible and latent heat loads for each room for a clay–straw wall and an internal mortar coating.

	Sensible load (kW h)			Latent load (kW h)		
	Living room	Bedroom 2	Bedroom 1	Living room	Bedroom 2	Bedroom 1
Non insulated roof	8062	3149	3160	1170	330	322
Red wood roof	7309	3023	3028	1173	335	327
White wood roof	7077	2966	2969	1173	336	328
Insulating panel 1	7016	2950	2952	1174	336	328
Insulating panel 2	6664	2865	2864	1179	338	330

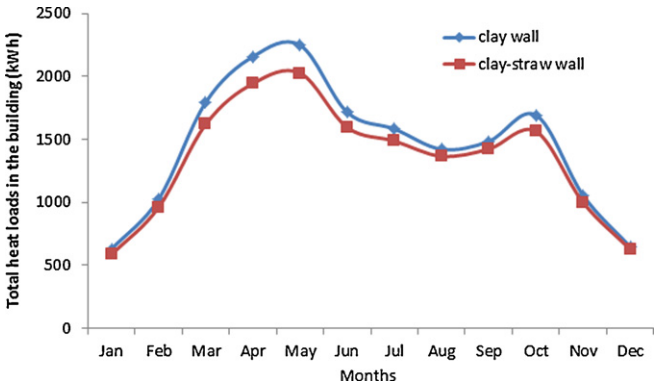

Fig. 5. Impact of the addition of straw in wall on the thermal load.

−17.3%. However, for bedroom 2, the relative differences range from −4.0% to −9.0%, and −4.17% to −9.36% for bedroom 1. Latent heat gains vary only slightly depending on the type of roof. Note finally that the latent heat in the living room is almost the same no matter which roof is used.

Fig. 7 shows the monthly thermal loads in the building for a clay–straw wall while the external surface is coated with a thin concrete layer and the interior involves an extra thin clay layer.

In this case, the relative differences between the reference case (straw–clay and non-insulated roof) with clay internal coating and other cases vary between 6.8% and 13.1% for April and between 6.3% and 12.1% for the month of May. These values change to between 6.9% and 13.4% for April and between 6.4% and 12 4% for the month of May for the case with internal mortal coating and vary between 6.9% and 11.4% for April and between 5.4% and 10.4% for the month of May for the reference clay wall and non-insulated roof.

As expected, the months of April and May, the hottest of the year (average maximum temperature of 41.8 °C and 41.6 °C, respectively) are those for which the overall heat gains are the largest and, consequently, the cooling loads are the greatest. It is also important to note that the solar flux is at its maximum in Ouagadougou during these two months. That is:

- April: total heat flux = 5698 W m^{-2} d^{-1}, direct flux = 3448 W m^{-2} d^{-1}, diffuse flux = 2250 W m^{-2} d^{-1}
- May: total heat flux = 5674 W m^{-2} d^{-1}, direct flux = 3313 W m^{-2} d^{-1}, diffuse flux = 2362 W m^{-2} d^{-1}.

A preliminary economic analysis indicates that the period of return on investment for adding insulation panel 2 is about 3 years while it turns out to be 5 years for the red wood roof. Under these circumstances, it would be advantageous to increase the thickness of the insulation to increase the net energy savings over the lifetime of the building. However, we did not attempt to optimize these values as other researchers did [19–23].

Other avenues, potentially more promising, for reducing thermal loads have not yet been explored. For example, using a white coating on the roof [24,25], or adding an air gap in walls and roof [22] as well as improving thermal insulation of windows could be more cost effective. In addition, in hot climates, there is the possibility of over-insulating a building, which traps the internal heat and accordingly, increases the cooling loads [26]. While this is not the case in the actual building configuration, since dominant heat load are external one, this could become a problem with improved insulation.

This is why using free cooling from forced or natural convection could be a viable option [6,27–30]. It should be noted that for passive systems, most of the time winds are weak in Ouagadougou, which limits their effectiveness. Strong winds, harmattan, do occur, but in cold month and bring a lot of dust that force to close every opening. Nevertheless, this might be a better option in other tropical climate.

All these options were out of the scope of the actual project as its goal was to investigate intervention that could be used as a retrofit of existing buildings or with a very minimal modification of the existing construction practice. As highly reflective paint may a

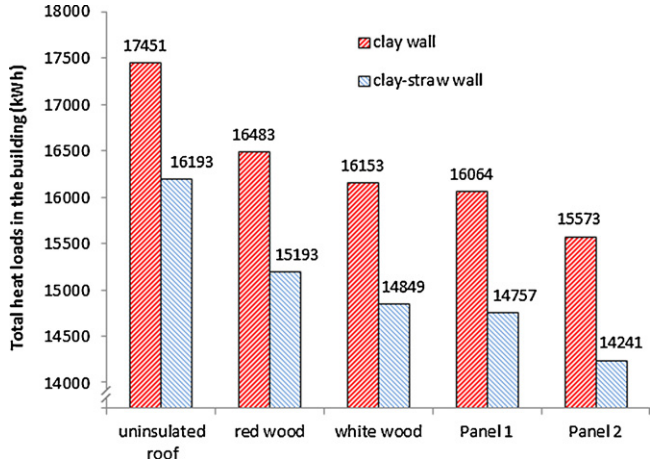

Fig. 6. Impact of roof insulation of thermal loads for the two walls configurations.

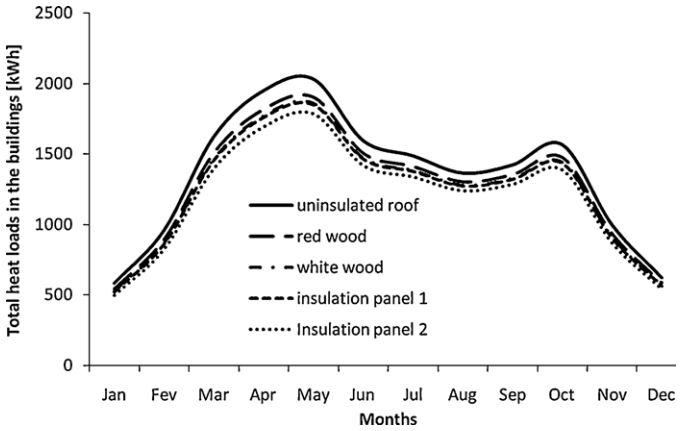

Fig. 7. Monthly heat loads for each building configuration.

priori seem to be ideal, this coating would not work out on long term basis as evidenced by the controversial paper published by Jacobson and Hoeve from Stanford University [31] in 2012. In consequence, the optimization of the insulation will have to await the results of future studies on these approaches, since it must be part of an integrated analysis.

5. Conclusion

This paper presents a study aimed at estimating the influence of local materials used for roof insulation on cooling loads of a typical clay–straw house. At first, the thermophysical properties (conductivity, thermal effusivity, density) of these materials were determined using a hot plate method with an analysis of thermograms in steady and unsteady regimes. The results obtained, while not directly comparable, are in the same range as those reported in the literature.

In the second part of this work, TRNSYS simulations indicated that the clay–straw wall consumes an average of 8% less energy than the standard clay wall on an annual basis. Then, the study highlights the influence of roof insulation on cooling loads. It has been shown that insulation only 1.5 cm thick can provide savings of up to 6.2% (red wood based house) to 12.1% (panel 2 based house) on cooling loads. Finally, the investigation indicates that differences in cooling loads due to the use of an interior clay coating in comparison with the concrete coating are negligible (0.24% on average). It has also been noted that the economic efficiency of insulation made from local materials is good. Still further thermo-economic optimization of the insulation thickness should be explored. In addition, researches are ongoing to determine the ideal clay–straw mix to minimize the cooling loads as an additional method to improve the overall insulation.

While this analysis has been carried specifically for a house situated in Ouagadougou, Burkina Faso, these techniques could be adapted and implemented successfully in others subtropical region where the construction technique are similar.

Acknowledgements

The first author (DT) wishes to thank Jean-Hugues Thomassin for the insulating panels which he oversaw the formulation and design of and his willingness to send them to Burkina Faso for their characterization in LPCE. The first author would also like to thank Frédéric Kuznik from Centre de Thermique de Lyon (CETHIL) for the license and the guidance offered on TRNSYS. The authors would finally like to thank the partners of the Industrial Research Chair in Energy Technologies and Energy Efficiency and the Natural Sciences and Engineering Council for funding the research group.

References

[1] DGE, Direction Générale de l'Énergie Audit Énergétique, et Stratégie Énergétique Domestiques (SED), Ministère de l'Énergie et des Mines du Burkina Faso, 2003.
[2] K. Baumert, M. Selman, Data note: heating and cooling degree days, in: Climate Analysis Indicators Tool (CAIT), World Resources Institute, Washington, DC, 2003.
[3] Intergovernmental Panel on Climate Change (IPCC), in: Solomon, et al. (Eds.), Climate Change 2007: The Physical Science Basis Summary for Policymakers, 2007.
[4] Institut de l'énergie et de l'environnement de la francophonie (EIPF), Les systèmes de ventilation et de climatisation, Fiches Techniques PRISME, 2001. http://www.iepf.org/media/docs/publications/97_climatisation.pdf (accessed on 15.02.12).
[5] Institut de l'énergie et de l'environnement de la Francophonie (IEPF), Efficacité énergétique de la climatisation en région tropicale, Tome 1: Conception des nouveaux bâtiments, PRISME, 2002. http://www.iepf.org/docs/prisme/eeTOME1.PDF (accessed on 15.02.12).
[6] I. Ouédraogo, et al., Modelling of a bioclimatic roof using natural ventilation, International Scientific Journal for Alternative Energy and Ecology (ISJAEE) 6 (2008) 106–110.
[7] B.A. Jubran, S.M. Habali, M.A.S. Hamdam, A.I.O. Zaid, Some mechanical and thermal properties of clay bricks for the Jordan valley, Material and Structures/Matériaux et constructions 21 (1998) 364–369.
[8] Y. Jannot, A. Zoubir, A. Kanmogne, Transient hot plate method with two temperature measurements for thermal characterization of metals, Measurement Science and Technology 17 (2006) 69–74.
[9] J.L. Izard, Construire avec le climat réunionnais, ENSA-Marseille, p. 11, http://www.envirobat-reunion.com/IMG/pdf_Construire_a_La_Reunion_1A.pdf (accessed 15.02.12).
[10] A.C. Kouchade, Détermination en routine de la diffusivité massique dans le bois par méthode inverse à partir de la mesure électrique en régime transitoire, Thèse de doctorat de l'ENGREF, Nancy France, 2004.
[11] S. Goodheew, R. Griffiths, Sustainable earth walls to meet the building regulations, Energy and Building 37 (2005) 451–459.
[12] H. Binici, O. Aksogan, T. Shah, Investigation of fiber reinforced mud brick as a building material, Construction and Building Material 19 (2005) 313–318.
[13] F.F. Al-ajmi, V.Q. Hambi, Simulation of energy consumption for Kuwaiti domestic buildings, Energy and Buildings 40 (2008) 1101–1109.
[14] M. Annabi, A. Mokhtari, T.A. Hafrad, Estimation des performances énergétiques dans le contexte maghrébin, Revue des énergies renouvelables 9 (2) (2006) 99–106.
[15] Adrian Shariah, Brhan Tashtoush, Akram Rousan, Cooling and heating loads in residential buildings in Jordan, Energy and Buildings, 26 2 (1997) 137–143.
[16] U. Diez-Webster, et al., Modélisation d'une maison à énergie positive, Projet de fin d'études, INSA, Lyon, 2006.
[17] S.A. Klein, et al., TRNSYS Version 16: User Manual, Solar Energy Laboratory, University of Wisconsin, 2006.
[18] B. Givoni, Building design principles of hot humid regions, Renewable Energy 5 (2) (1994) 908–916.
[19] A. Bolattürk, Determination of optimum insulation thickness for building walls with respect to various fuels and climate zones in Turkey, Applied Thermal Engineering 26 (2006) 1301–1309.
[20] A. Bolattürk, Optimum insulation thicknesses for building walls with respect to cooling and heating degree-hours in the warmest zone of Turkey, Building and Environment 43 (2008) 1055–1064.
[21] J. Yu, C. Yang, L. Tian, D. Liao, A study on optimum insulation thicknesses of external walls in hot summer and cold winter zone of China, Applied Energy 86 (2009) 2520–2529.
[22] N. Daouas, A study on optimum insulation thickness in walls and energy savings in Tunisian buildings based on analytical calculation of cooling and heating transmission loads, Applied Energy 88 (2011) 156–164.
[23] N. Sisman, E. Kahya, N. Aras, H. Aras, Determination of optimum insulation thicknesses of the external walls and roof (ceiling) for Turkey's different degree-day regions, Energy Policy 35 (2007) 5151–5155.
[24] A. Synnefa, M. Santamouris, H. Akbari, Estimating the effect of using cool coatings on energy loads and thermal comfort in residential buildings in various climatic conditions, Energy and Buildings 39 (2007) 1167–1174.
[25] A. Bhatia, J. Mathur, V. Garg, Calibrated simulation for estimating energy savings by the use of cool roof in five Indian climatic zones, Journal of Renewable and Sustainable Energy 3, 023108_2011, http://link.aip.org/link/doi/10.1063/1.3582768, in press.
[26] O.T. Masoso, L.J. Grobler, A new and innovative look at anti-insulation behaviour in building energy Consumption, Energy and Buildings 40 (2008) 1889–1894.
[27] B.R. Hughes, H.N. Chaudhry, S.A. Ghani, A review of sustainable cooling technologies in buildings, Renewable and Sustainable Energy Reviews 15 (2011) 3112–3120.
[28] C. Inard, J. Pfafferott, C. Ghiaus, Free-running temperature and potential for free cooling by ventilation: a case study, Energy and Buildings 43 (10) (2011) 2705–2711.
[29] C. Ghiaus, F. Allard, Potential for free-cooling by ventilation, Solar Energy 80 (4) (2006) 402–413.
[30] E. Shaviv, Design tools for bio-climatic and passive solar buildings, Solar Energy 67 (1999) 189–204.
[31] M.Z. Jacobson, J.E. Ten Hoeve, Effects of urban surfaces and white roofs on global and regional climate, Journal of Climate 25 (3) (2012) 1028–1044.